Lead-Free Electronic Solders 347–365

Impact of the ROHS Directive on high-performance electronic systems

Part II: key reliability issues preventing the implementation of lead-free solders

Karl J. Puttlitz · George T. Galyon

Published online: 22 September 2006
© Springer Science+Business Media, LLC 2006

Abstract There are important logistical and technological issues that confront the electronics industry as a result of implementing lead (Pb)-free technology to comply with the European Union's (EU) ROHS Directive effective July 1, 2006. This paper focuses on the technological matters that pose the greatest potential risk to the reliability of so-called high-performance (H-P) systems (i.e., servers, storage, network infrastructure/telecommunication systems). The European Commission (EC) specifically granted a special use of lead (Pb) in solder exemptions, independent of concentration, for applications in H-P systems. The intent was to preserve the reliability of solder joints, particularly flip-chip solder joints. H-P systems perform mission-critical operations, so it is imperative that they maintain continuous and flawless operation over their lifetime. H-P systems are expected to experience virtually no downtime due to system failures. This paper discusses several major technological issues that impede the implementation of Pb-free solders in H-P systems. The topics discussed include solder compatibility and the reliability risks of mixed solder joints due to component availability problems. The potential effects of microstructural factors, such as the presence of Ag_3Sn platelets, and ways to eliminate them are described. Also discussed are the effects that stress-test parameters have on the thermal-fatigue life of several Pb-free solders compared to eutectic Sn–Pb. Another issue discussed involves the effect that tin's body-center tetragonal (BCT) crystal structure has on solder-joint reliability, and the complete loss of structural integrity associated with an allotropic phase transformation at 13.2°C, referred to as tin pest. Yet another important consideration discussed is the tendency of pure tin or tin-rich finishes to grow "whiskers" that can cause electrical shorts and other problems. Finally, the paper notes the potential for electromigration failures in Pb-free, flip-chip solder joints. Based on the current status of the issues discussed, it appears likely that the exemption allowing the use of lead (Pb) in solder will need to be extended by the EC when scheduled for review in 2008, and perhaps well into the future.

K. J. Puttlitz (✉)
Puttlitz Engineering Consultancy, LLC, Wappingers Falls, NY 12590, USA
e-mail: KJPuttlitz@aol.com

G. T. Galyon
IBM eSystems and Technology Group, Poughkeepsie, NY 12601-5400, USA
e-mail: Galyon@us.ibm.com

1 Introduction

The European Union (EU) legislation, "Restriction of the Use of Certain Hazardous Substances (ROHS) in Electrical and Electronic Equipment" (Directive 2002/95/EC) effectively bans the use of lead (Pb) and several other substances in electrical products. This paper contains references to "lead-free" solder alloys which has become an industry-standard term meaning that the solder should contain less than the ROHS Directive limit of 0.1 wt% (1,000 ppm) for lead (Pb). It does not mean that the solder alloy will necessarily contain no lead (Pb) at all. The worldwide effort to eliminate the banned substances, particularly Pb, has surfaced some significant logistical and technical challenges to

the electronics industry. How to disposition Pb-bearing inventory? How to easily distinguish and maintain separation of converted and Pb-bearing parts to avoid confusion and costly errors on the manufacturing floor? What due diligence procedures should be followed to assure compliance and avoid potentially severe legal repercussions? How to establish the necessary supply-line partnerships and controls to assure the continuous availability of truly compliant parts? While these logistical matters are important it is the technology-based issues that pose the greatest concern due to their potential impact on reliability. No widely accepted ''drop-in'' Pb-free solder replacement for eutectic Sn–Pb has been identified as yet. Only sparse laboratory test data was initially available for the several Pb-free solder candidates being evaluated across the global electronics industry, and the melting point for most of the lead-free solders is about 30°C higher than the melting point of eutectic Sn–Pb. In addition, it has not been possible to infer reliability performance for the lead-free solders from the existing Sn–Pb reliability data base because the metallurgical characteristics of high-lead content and eutectic Sn–Pb solders are significantly different compared to Pb-free solders. Based on these considerations the EC provided several solder-usage exemptions when the legislation was initially enacted and since then has granted several additional exemptions requested by the electronics industry. From the outset the EC recognized that there was a special class of electronic products (e.g., servers, storage, network infrastructure/telecommunications equipment) used in mission-critical operations whose operational integrity and reliability had to be preserved. Reliability greatly depends upon individual solder joint integrity. Of particular concern are flip-chip solder joints owing to their importance in high-performance circuits and the harsh mechanical conditions they must endure: e.g., exposure to repeated shear stress fluctuations resulting from the coefficient of thermal expansion (CTE) mismatches between the materials on either side of the solder joint. The EC did not provide a permanent exemption for the use of Pb in solder for high-performance products, but did agree to review the matter every 4 years starting in 2008. Another reliability concern is associated with the implementation of lead-free solder attachments involves the mixing of leaded and lead-free solders. During the initial transition phase it will be inevitable that electrical components with leaded (Pb) solders on their attachment points will be used in lead-free, solder-attachment processes. Mixed-solder joints can result in severe reliability problems. Several other significant technical issues existed at the time the legislation was enacted that also helped prompt the EC to grant the continued use of lead (Pb) in solder exemption. While progress has been made in some cases, in others the problems are inherent and must be sufficiently characterized in order to determine if a ''safe'' operating condition or window can be established. For example, the wettability of all the most popular Pb-free solder candidates is less than Sn–Pb. There are solidification peculiarities associated with Sn–Ag–Cu or SAC alloys that can result in the presence of large Ag_3Sn platelets randomly oriented throughout the microstructure under conditions similar to those often encountered during manufacturing. The thermo-mechanical fatigue characteristics for SAC solders have been found to be very different compared to Sn–Pb solders. There are several other lead-free solder issues that did not exist with Pb–Sn solders which are directly related to tin's crystal structure. Pure tin undergoes a phase change at about 13°C that results in a condition called ''tin pest'' that literally causes the tin to disintegrate structurally into a dust-like powder. Still another very serious reliability concern is the tendency for tin electroplated finishes to form filamentary growths called whiskers. These whiskers are conductive and have caused electrical shorting in several mission critical applications involving heart pacemakers, space capsules, and missile control systems. For many decades lead has been added to electroplated tin finishes to mitigate or reduce the tendency to form whiskers. The elimination of lead will, unless otherwise mitigated, significantly increase the risk of whisker shorting failures. Finally, solder-joint electromigration resistance is becoming increasingly more important due to increased electrical current levels associated with high-performance electrical circuits.

2 Mixed solder joints

2.1 Reliability implications due to parts availability

The ROHS lead elimination directive will have a significant impact even for those manufacturers (e.g. medical, military, server, telecommunication, storage) whose products are permitted continued usage of leaded (Pb) solders. Manufacturers who purposely choose not to be compliant will also be impacted. The high volumes associated with parts utilized in certain consumer-electronic products will dictate that a particular component is solely manufactured as a Pb-free version [1, 2]. The demand for most Pb-free part numbers will be so great in relation to their leaded counterparts

that many suppliers will elect not to support both lead (Pb)-bearing and lead-free versions of the same parts. Some suppliers (e.g., Infineon) have stated plans to continue providing leaded products to customers whose markets allow them to use lead-bearing parts [3]. Shortages of some Pb-free part numbers are anticipated early on presenting consumer-electronic manufacturers with product development and market introduction challenges that will eventually dissipate [4]. More serious will be the unavailability of some key Pb-bearing parts by manufacturers of high-performance products who plan to invoke the exemptions provided to assure the reliability of those products as intended, or entities that simply wish to remain non-compliant. Some degree of mixed (i.e., hybrid) metallurgical solder joints raises the potential for serious reliability problems. This situation is particularly ironic because the reason for granting the lead-usage exemptions was because of the uncertainty associated with the reliability of Pb-free solder joints [5]. The currently available reliability data base for hybrid solder joints is even more scant than that for lead-free solders.

2.2 Component and process compatibility

There are eight solder joint types that can be created during solder reflow operations (Table 1) as a result of solder composition variations between the component attachment point (i.e., lead-frame finish or solder ball) and the solder paste.

No compositional issues are introduced in cases involving component lead finishes or solder balls and solder paste of the same composition assuming the solder joints are formed utilizing an adequate reflow-temperature profile. A lead (Pb)-free component is said to be backward compatible if it can be reliably joined to a PCB utilizing eutectic Sn–Pb solder with a standard Sn–Pb reflow-temperature profile. Similarly, a Sn–Pb component is said to be forward compatible if it can be reliably reflowed to a PCB using a Pb-free solder paste and a Pb-free reflow temperature profile. Both forward and backward compatibility can be achieved for both Sn–Pb and Pb-free components (Table 1) and such processes are practiced by many major manufacturers [6, 7].

2.3 Forward compatibility

The forward-compatible lead-frame products with Pb-based finishes are virtual drop-in replacements for their Pb-free counterparts. But some caution must be exercised. Pb-based components are designed to withstand Sn–Pb reflow process temperatures, typically with a maximum 230°C rating. Component manufacturers have made appropriate material changes such that, Pb-free components are capable of withstanding the significantly higher Pb-free process temperatures. So care must be exercised in assuring that the reliability of a Pb-bearing component is not compromised when subjected to the higher temperature (235–260°C) utilized for a Pb-free reflow process. Care must also be exercised in selecting a Pb-free solder paste that is metallurgically compatible with lead (Pb) [8]. For example, Pb-free solders containing bismuth (Bi) can form a low-melting compound in the presence of Pb that very significantly reduces the maximum-allowable application temperature. Bismuth-containing solders are successfully utilized by limiting the bismuth content to about 5% maximum. Some manufacturers who favor bismuth solders due to their relatively low melting points in comparison to the more commonly used SAC solders. Lead-free solder paste compositions vary considerably with respect to the various elements combined with Sn, Cu, Ag, Bi, In, Bi and others.

2.4 Backward compatibility

2.4.1 Lead-frame components

Generally speaking manufacturers have found that most lead-free surface finishes on lead-frame components are fully backward compatible with Pb–Sn solder and will not cause soldering or reliability problems [9] in spite of their higher melting points. The thin plating dissolves into the molten Pb–Sn solder volume, providing backward compatibility. However, depending on the joint solder volume, it is sometimes necessary

Table 1 Solder joint variations

Component		Solder paste and reflow utilized	
Termination	Solder	Lead (Pb) free	Tin–lead
Lead finish	Sn–Pb	Hybrid (forward compatible)	Homogenous
Lead finish	Pb-free	Homogeneous	Hybrid (backward compatible)
Ball	Sn–Pb	Typically not forward compatible	Homogeneous
Ball	Pb-free	Homogeneous	Typically not backward compatible

Note: The reflow temperature range for eutectic Sn–Pb is typically between 220 to 235°C and 235 to 260°C for Pb-free solder pa1stes

to slightly increase the peak reflow temperature to achieve good-quality solder joints [7]. Backward compatibility covers a variety of lead-frame components: TQ, PQ, UQ, SO, VO, SOIC, PLCC, QFP, etc [10, 11]. It offers a valuable solution to manufacturers utilizing a Sn–Pb assembly process who must incorporate one or more lead-free components. They can do so with no adverse affect on reliability with only minor changes in the assembly process [10].

2.4.2 Solder ball terminals (ball grid arrays or BGAs)

As noted, the hybrid solder joints resulting from plated lead-free lead-frame components are generally considered a low reliability risk. But in the case of Pb-free ball grid array (BGA) terminations the joint reliability depends upon the homogeneity of the microstructure as a result of the reflow conditions. The issue here is that the melt temperature of the Pb-free solder balls is significantly greater than that for eutectic Sn–Pb solder paste. For example, Sn–Ag–Cu (SAC 305) melts at approximately 217°C vs. 183°C for eutectic Sn–Pb. As a result, the solder spheres either partially melt or do not melt at all during the Sn–Pb reflow process [2]. In general, it has been demonstrated that if the reflow results in an inhomogeneous solder joint due to only a partial melting of the solder ball, the solder joints exhibit a much-reduced reliability compared to standard eutectic Sn–Pb BGA solder joints [12–15]. Incomplete melting of the solder ball can cause poor self-alignment, open solder joints, and latent defects [15]. Conversely it was demonstrated for a wide range of components with Sn–Ag–Cu solder balls, if the peak reflow temperature was > 217°C and the time above liquidus (183°C) was sufficiently long, complete melting and mixing was observed in the solder joints of CSPs [12, 13], PBGA-196, 256 [15], and CBGA-937 components [14, 15]. These studies have shown that the reliability of some fully mixed and homogeneous solder joints are equivalent to or better than comparable Pb–Sn joints. Although some joints were observed to be statistically worse than their Pb–Sn counterparts, they were judged to not pose a severe reliability risk compared to the high reliability risk of joints with partially melted Sn–Ag–Cu solder balls [13]. Interestingly, the failure modes of both fully and partially reflowed BGA solder joints in accelerated thermal cycle (ATC) tests were observed to be the same. Cracks initiated at the component/solder interface and propagated through the region with coarsened grains, i.e., areas of high stress concentration. The lower fatigue life of partially mixed solder joints was attributed to a reduced ability of an inhomogeneous microstructure to dissipate the stress [15]. Unfortunately, to achieve consistently homogeneous solder joints requires utilizing either a lead-free or higher than normal tin–lead reflow profile. The higher temperature itself has its own potential for reliability problems associated with degraded component and PCB materials.

Adjustments in reflow parameters may be necessary based on ball size and composition since they play a significant role in mixing kinetics. Large BGA balls require longer times and higher temperatures to adequately mix with Sn–Pb solder. SAC305 solder balls require a 3–5°C higher reflow temperature than SAC405 solder alloys. Under the same reflow parameters (peak temperature, time above liquidus, and solder paste/solder joint ratio) the mixed portion of the solder joint is smaller in size for SAC305 compared to SAC405 [15]. In addition, excessive voiding has been observed in BGA solder joints based both on size and composition. For example, voids were observed to occur within 1.0-mm and finer pitch BGA balls, but to only occur minimally with larger pitches (e.g., 1.27 mm). The cause of the voids is not understood given that soak times of 60–120 s are normally ample to allow flux volatiles to escape prior to solder reflow [9]. The incidence of voiding was noted to be least for BGA solder joints constructed from SAC405 solder balls and paste, increasing with a mixture of SAC405 balls/SAC305 paste, and worst for a mixture of SAC405 balls/Sn–Pb paste. The pure Pb-free joints were reflowed at 235–245°C, while the mixed solder joints were reflowed at a 220°C peak temperature [14].

2.5 Processing

2.5.1 Pb-free finished lead frame components

As indicated in Fig. 1, a standard Sn–Pb profile can be utilized to reflow attach Pb-free finished lead-frame components. The optimum profile depends upon additional factors such as component mass and distribution (i.e., layout) on a board, board size, geometry, etc. Semiconductor suppliers (e.g., National Semiconductor) are recommending that board-level assemblers adopt J-STD-020C to establish an industry-wide reflow standard [16]. Owing to their backward compatibility Pb-free finished lead-frame components can be utilized along with Pb-based components without the need to alter the standard Sn–Pb assembly process [8].

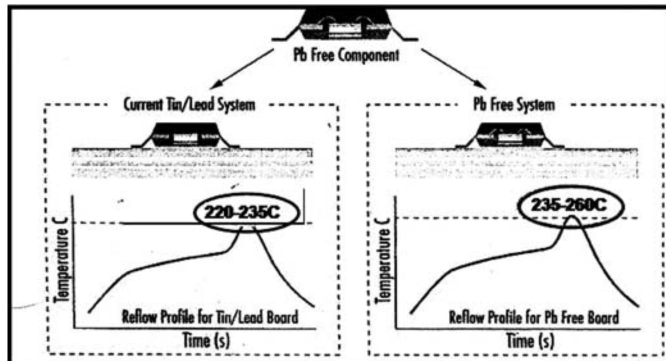

Fig. 1 Schematic depicting temperature profiles for reflow attaching Pb-free finished lead-frame components with either Sn–Pb or Pb-free solders (after Ref. [10])

2.5.2 Pb-free solder ball (BGA) terminated components

The predominant position in the industry has been not to create mixed BGA solder joints consisting of Pb-free solder balls and eutectic Sn–Pb solder paste, because as has been noted earlier, the resulting inhomogeneous solder joint created by standard Sn–Pb reflow conditions exhibits unacceptable fatigue characteristics. However, the realities are that in many instances it will be almost impossible to avoid Pb-free BGA mixed solder joints in an assembly. Although the options are limited, these joints can be made to be backward compatible. The most desirable solution, although rarely available, is to reball the components with Sn–Pb solder balls [9]. In the absence of that capability, steps must be taken to determine the profile conditions (peak temperature, dwell time) that have the least detrimental effects on the assembly materials and still capable of producing fully mixed and homogeneous solder joints. Acceptable ATC test results must confirm the adequacy of the mixed solder joints.

High-performance systems manufacturers will in the main continue to use eutectic Sn–Pb to assemble their PCBs. It will be inevitable that some components are only available with lead-free terminations. Lead-free, lead-frame components generally are not a concern since they can be assembled utilizing standard Sn–Pb processes (i.e., they are backward compatible). But lead-free BGA components will be a source for concern since they are not backward compatible. In some instances it will be possible to achieve compatibility through process and material modifications, while in other cases it may not be viable to do so.

3 Reduced wetting characteristics of Pb-free solders

A variety of Pb-free solders have been investigated as replacements for eutectic Sn–Pb solder. None of them can be considered as a "drop-in" replacement for eutectic Sn–Pb. For reflow applications the consensus lead-free solder choice is a near-ternary eutectic Sn–Ag–Cu alloy with, in some cases, relatively minor additions of other elements. A comprehensive review of Sn–Ag, Sn–Cu, Sn–Ag–Cu, Sn–Ag–Cu–X, and Sn–Ag–X solders and solder joints is available in the literature [17, 18]. Some unique Sn–Pb solder attributes have made the search for a Pb-free system with similar characteristics difficult. Sn–Pb is a binary eutectic system with only one chemically active constituent, tin (Sn). All the chemical bonds that Pb–Sn solders form do so by the creation of intermetallic compounds (IMCs) containing only Sn. However, lead (Pb) does play an important role by providing molten Sn–Pb solders with a low surface tension value that is a major contributing factor to the excellent solderability (i.e., wetting and spreading) characteristics exhibited by Sn–Pb solders [19]. For example, the surface tension of molten Pb is 450 dynes/cm (at $T_{melt} = 326°C$), and molten Sn is 550 dynes/cm (at $T_{melt} = 232°C$). The wetting characteristics of eutectic Sn–Pb exceed those of all Pb-free solders of current interest when soldered to the base metals typically utilized in electronic assemblies (Figs. 2, 3). Minor elemental additions of Ag, Bi, Cu, In, Sb, Zn, etc. are used to lower the melt temperature and to enhance the mechanical properties of many lead-free solders. However, these alloy additions also significantly degrade solderability characteristics. Consider for example the binary solder Sn–58Bi utilized for applications requiring good wettability and a low-melt temperature. As shown in Fig. 4, a 1% addition by each of several alloying elements results in a moderate-to-significant loss in wettability (i.e., higher contact angle). The reliability implications related to reduced wetting characteristics is an unknown. This is just another example from a long list of technology concerns associated with the implementation of lead-free solders for high-performance systems assembly operations.

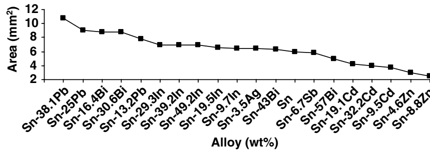

Fig. 2 Comparative spreading area measurements for several lead-bearing and lead-free solder alloys on copper utilizing a resin flux. Near-eutectic Sn–Pb exhibited better wetting (i.e., greatest spreading area) compared to all Pb-free alloys tested (after Ref. [20]) (courtesy of CRC Press)

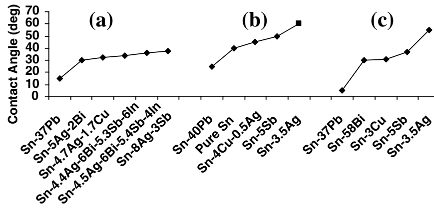

Fig. 3 Equilibrium wetting contact angles of several Pb-free solder alloys under various reflow conditions. (**a**) Cu substrate with RMA (GF-1235) flux (from Drewin et al. [21]). (**b**) Cu substrate with RMA (Alpha 611) flux ~40°C superheat over the liquidus temperature (from Vianco et al. [22]). (**c**) Cu substrate with RMA flux at ~30°C superheat over the liquidus temperature where the liquid alloy is dispensed onto a heated substrate (from Pan et al. [23]). Eutectic or near-eutectic Sn–Pb exhibits better wetting (i.e., lowest contact angle) compared to all Pb-free solders tested, under all test conditions (courtesy of CRC Press)

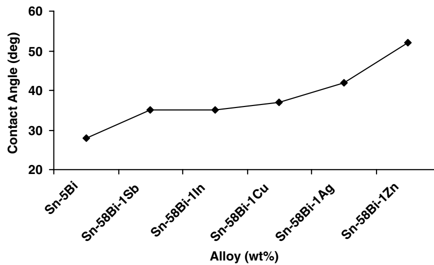

Fig. 4 Comparison of the contact angles of eutectic Sn–Bi and individual 1% ternary element additions when reflowed on Cu at a 200°C peak reflow temperature and using Kester 197 rosin flux. In each case a 1% ternary addition resulted in reduced wettability (i.e., increased contact angle) compared to the binary Sn–58Bi solder alloy (from Ref. [24], courtesy of CRC Press)

4 Solidification and microstructure of near-eutectic Sn–Ag–Cu alloys

4.1 Highly non-equilibrium structure

The Sn–Ag–Cu eutectic composition is thought to be Sn–3.5Ag–0.9Cu with a eutectic melting point at 217°C [25, 26]. Some commercially available, near-eutectic alloys are: Sn–4.0Ag–0.5Cu and Sn–3.8Ag–0.7Cu. These near eutectic Sn–Ag–Cu alloys consist of three phases (β-Sn, Ag_3Sn and Cu_6Sn_5) that form immediately upon solidification from the liquid state. Both the Ag_3Sn plates and Cu_6Sn_5 rods formed are intermetallic compound phases. However, none of the phases are present in the amounts predicted by the equilibrium phase diagram since they are not formed as an equilibrium microstructure. The intermetallic compound (IMC) phases nucleate and grow with minimal undercooling. These pro-eutectic phases may undergo excessive growth under slow-cooling conditions due to the fact that they continue their growth from the liquid state until the molten solder has been sufficiently undercooled by 15–30°C. Undercooling is required to nucleate β-Sn crystals from the liquid phase. By comparison tin–lead based solders only require a small amount of undercooling to initiate solidification. Once β-Sn nucleates solidification occurs very rapidly with a dendritic morphology. A typical Sn–Ag–Cu solder joint substantially solidifies in less than a second after β-Sn nucleation commences and with β-Sn dendrites forming more than 90 wt% of the solder joint [27]. The eutectic intermetallic phases (Ag_3Sn and Cu_6Sn_5) nucleate simultaneously from the liquid located between impinging β-Sn dendrites. These IMC phases are manifested as fine-precipitate particles that outline the dendritic β-Sn grain's structure. The microstructure of a slow-cooled BGA solder ball depicted in Fig. 5 is typical of the highly non-equilibrium structure formed as a result of the events described. The dendritic β-Sn structure noted is very evident in Fig. 6. It was observed that as-solidified BGA solder joints approximately 900μm (0.035 in.) in diameter are typically composed of 1–10β-Sn grains [28], with an average of about eight grains. The small number of grains, together with the anisotropy of β-Sn, are reasons to anticipate mechanical property variations for Pb-free solder joints. The reliability impact from these mechanical property variations is, as yet, unknown.

4.2 Ag_3Sn plates

4.2.1 Observed effects

The presence of Ag_3Sn platelets were reported to have adverse effects on the plastic deformation properties of solidified solder joints [29]. Henderson et al. [28] subjected BGA solder joints to thermo-mechanical testing (0–100°C) and observed strain localization and large strains due to grain boundary sliding at the boundary between the Ag_3Sn and β-Sn phases. The orientation

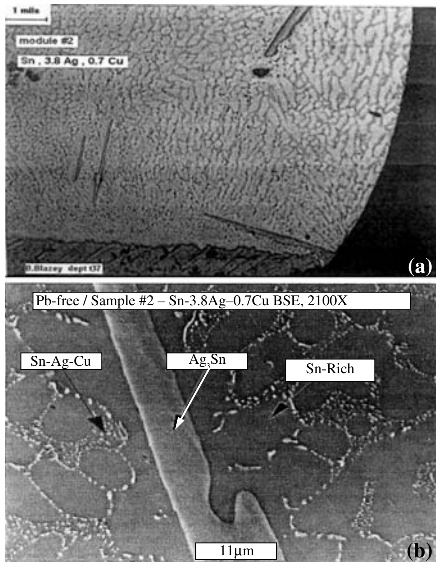

Fig. 5 SEM micrograph showing the typical microstructure of a slow-cooled Sn–3.8Ag–0.7Cu alloy in a BGA solder ball at two magnifications. The tin dendritic arms (light appearing phase) in (**a**) are surrounded by Ag_3Sn and Cu_6Sn_5 particulates as is clearly evident in (**b**) that decorate the β-Sn phase (after Ref. [27])

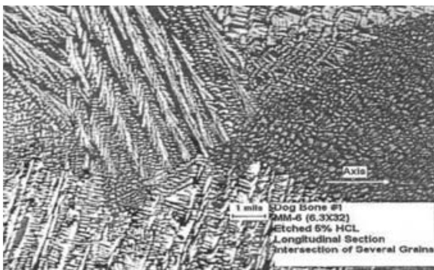

Fig. 6 Scanning electron microscope (SEM) image of a slow-cooled test sample of Sn–3.8Ag–0.7Cu solder alloy lightly etched to reveal the dendritic growth structure of the β-Sn phase (after Ref. [27])

of some plates were conducive to causing the top portion of some solder joints to shift relative to the lower portion as shown in Fig. 7. Strain localization at the β-Sn/Ag_3Sn boundary was also observed earlier by Frear et al. [30].

4.2.2 *Factors that control Ag_3Sn plate formation*

Extensive studies were conducted [28, 31, 32] to determine the controlling factors for Ag_3Sn platelet

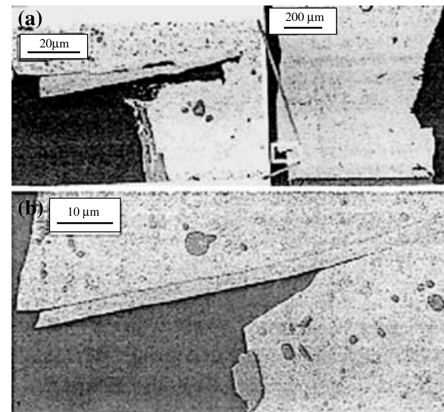

Fig. 7 Vertical cross-section view of two solder joints that exhibit large strains localized at the boundary between a Ag_3Sn plate and β-Sn phase subsequent to an accelerated thermal cycle (ATC) test conducted at 0–100°C. The top portion of the solder joint has shifted in relation to the bottom portion along the Ag_3Sn/β-Sn boundary in each of these joints (after Ref. [28])

formation in near-eutectic Sn–Ag–Cu solder alloys. Of interest was the relationship between typical joint assembly cooling rates (0.2–4.0°C/s) and Ag_3Sn platelet formation. Results showed that cooling rate had a significant effect on Ag_3Sn platelet formation utilizing 0.88 mm diameter Sn–3.8Ag–0.7Cu BGA solder joints mounted on electroless Ni/immersion Au-plated pads on an organic chip carrier (Fig. 8). At low cooling rates ($<$ 1°C/s) Ag_3Sn platelets grow large enough to span the entire BGA cross-section. For cooling rates between 1.5 and 2.0°C/s the platelet size is much smaller than the solder joint dimension, and at very fast cooling rates ($>$ 3.0°C/s) platelet formation can almost be completely suppressed [28]. By conducting similar experiments with a hypoeutectic alloy, Sn–2.5Ag–0.9Cu (Fig. 9), it was determined that Ag content has a significant effect on Ag_3Sn plate formation. Results with this lower Ag content solder alloy showed that Ag_3Sn platelets rarely form, even at slow cooling rates; but that large Cu_6Sn_5 IMC rods appear [28]. Copper content was found to have only a minor effect on Ag_3Sn plate formation [31]. But lowering the Cu content is beneficial in reducing the so-called "pasty range"; the temperature range between the liquidus and solidus temperatures, where the equilibrium structure is a mixture of liquid and solid phases. Copper concentrations above the eutectic composition of 0.9 wt% in SAC alloys increases the pasty range [32]. Reducing the pasty range typically results in fewer solder joint defects, such as pad lifting of plated through holes (PTHs). A reduction in silver (Ag)

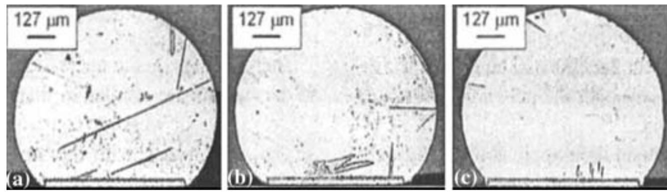

Fig. 8 Microstructure of Sn–3.8Ag–0.7Cu BGA solder balls cooled from a 240°C peak reflow temperature at various cooling rates. (**a**) 0.2°C/s, (**b**) 1.2°C/s, (**c**) 3.0°C/s (after Ref. [28])

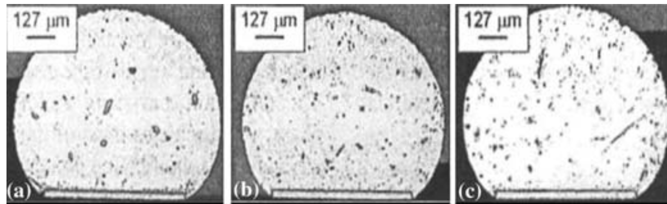

Fig. 9 Microstructure of Sn–2.5Ag–0.9Cu solder balls cooled from a 240°C peak reflow temperature at various cooling rates. (**a**) 0.2°C/s, (**b**) 1.2°C/s, (**c**) 3.0°C/s (after Ref [28])

content is the current preferred method for eliminating or minimizing Ag_3Sn platelet formation. Rapid cooling may not be possible or practical in a manufacturing environment due to such things as large variations in the size and thermal mass of components that result in the introduction of excessive stresses in some assemblies and their solder joints.

5 Fatigue properties of Pb-free solders

5.1 Shear stresses due to CTE mismatch

Thermal–mechanical fatigue resistance is among the most critical reliability concerns with the introduction of lead-free solder joints. The ability to withstand repeated deformations due to stresses generated by the CTE mismatches between materials at the opposite ends of solder joints is critical to the reliability of H-P electronic equipment. Flip-chip and BGA solder joints are particularly susceptible to thermal–mechanical fatigue failure because there are some large CTE differences amongst the materials that comprise these assemblies (Table 2). For example, flip-chip solder joints can experience moderate-to-severe thermally induced shear stresses depending on whether they are mounted on ceramic or organic (plastic) chip carriers. The situation is similar for BGA solder joints where the thermally induced stress levels also depend upon whether the carrier material is ceramic or organic. Thermal excursions result from machine power "on/off" cycling and from operating between full and reduced (i.e., sleep or rest) power modes utilized to conserve power.

5.2 Parameters that affect fatigue life

Numerous fatigue studies have been reported covering Pb-free solder joints for several types of mounted components exposed to a variety of stress conditions. Some studies show that Pb-free, solder-joint fatigue life far exceeds the fatigue life for standard eutectic Sn–Pb solder joints [33]. However, other studies show that eutectic Sn–Pb has superior fatigue life in comparison to lead-(Pb)-free solder joints. For example, the Sn–Ag–Cu solder joints of a 48-I/O TSOP and 2512-sized resistor cycled between 0–100°C, – 40–125°C, and –55–125°C [34] had a fatigue life significantly less than similarly tested eutectic Sn–Pb joints. Some of these seemingly contradictory results in the literature may be due to differences in the thermal-fatigue behavior of near-eutectic Sn–Ag–Cu solder alloys compared to eutectic Sn–Pb under various stress conditions. Such differences were very apparent in a fundamental study conducted by Bartelo et al.[35]. A comparison was made between the thermo-mechanical fatigue life of both Sn–3.8Ag–0.7Cu (SAC) and Sn–3.5Ag–3.0Bi (SAB) compared to eutectic Sn–Pb solder that served as a benchmark, using ceramic BGA modules attached to an organic card as a test vehicle. The initial test cycle investigated was 0–100°C and three cycle times: 30, 60, and 120 min. The accumulative failures in each case were plotted lognormally as a function of their thermal-cycle life, and then replotted to normalize all the data relative to the N_{50} value of the Pb–Sn solder joints, made to equal 1 for ease of comparison purposes (Fig. 10a). N_{50} represents the number of thermal cycles at which 50 percent of the test population failed, and was used as the comparison value among the three

Table 2 Coefficients of thermal expansion (CTE) values for materials of mounted BGA components

Material	Approximate CTE, ppm/°C
Silicon	3
Ceramic (Al_2O_3)	6
Plastic	16-22
Epoxy/Glass	16-22

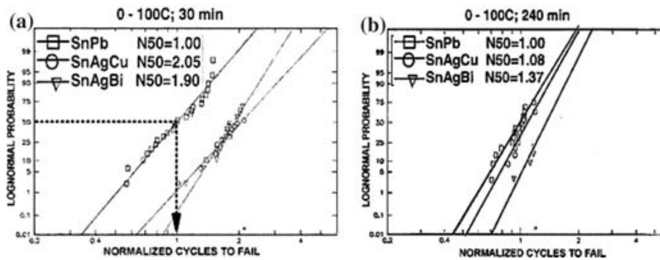

Fig. 10 Accelerated thermal cycle (ATC) test results comparing the thermo-mechanical fatigue life of two popular lead (Pb)-free solders (Sn–3.8Ag–0.7Cu or SAC, and Sn–3.5Ag–3.0Bi or SAB) in relation to eutectic Sn–Pb whose N_{50} was normalized to equal 1. The test conditions: 0–100°C cycle, cycle time (**a**) = 30 min, (**b**) = 240 min. (after Ref. [35])

solder compositions. For the 0–100°C/30-min. test condition, both the SAC and SAB alloys exhibited a fatigue life approximately two times better than Sn–Pb (2.05 and 1.9, respectively). For the longer 240-min. cycle the fatigue life of both Pb-free solders was markedly reduced with SAC nearly equivalent to Sn–Pb, and SAB only marginally better (Fig. 10b). Subsequently, the temperature cycle was altered to –40°C–125°C (a $\Delta T = 165$°C instead of 100°C). Both Pb-free alloys experienced further reductions in thermal fatigue life relative to Sn–Pb due to the increased temperature deltas and become worse with increased cycle time (see Table 3). For example, the comparative fatigue life of both Pb-free solders for the 240-min cycle time was SAC-73% and SAB-96%, with 100% representing equivalence with Sn–Pb. A final test was conducted to determine if an increased temperature range and/or an increased peak temperature was responsible for the loss in fatigue life, since both stress-test parameters were increased in the prior test. In the final test all test conditions utilized a constant cycle time = 30 min, and a constant temperature range (ΔT) = 100°C, but the peak temperature varied (60, 100 and 125°C). As noted on the right side of Table 3 both the SAC and SAB solders suffer a dramatic reduction in fatigue life relative to eutectic Sn–Pb with an increase in peak temperature.

5.3 Effect of cooling rate

Microstructure plays a significant role in determining solder joint mechanical properties. As previously

Table 3 Effect of temperature range, peak temperature, and cycle time on the fatigue life of two lead-free solders relative to Sn–Pb

Solder	Fatigue life relative to Sn–Pb				
	– 40°C to 125°C, ΔT = 165°C		30 min, ΔT = 100°C		
	4 Min	240 min	–40–60°C	0–100°C	25–125°C
Sn–Ag–Cu (SAC)	0.84	0.73	2.32	2.05	1.25
Sn–Ag–Bi (SAB)	1.21	0.96	2.93	1.90	1.12

Based on Ref. [35]

discussed, the solidification cooling rate has a large effect on the near-eutectic Sn–Ag–Cu solder microstructure. A study [36] addressed the effects these microstructural changes have on the fatigue life of SAC alloys. Ceramic BGA modules were mounted to organic cards with Sn–4.0Ag–0.5Cu solder paste. The Sn–Ag–Cu solder ball compositions ranged in Ag content from 2.1 to 3.8%. Parts from all compositions were cooled from a 240°C peak temperature at two rates, 0.5°C/s (slow) and 1.7°C/s (fast). The actual Ag composition of the reflowed solder joints was calculated to be slightly higher (by 0.15–0.2 wt%) than the BGA solder ball composition owing to the higher Ag content in the solder paste. Three ATC test conditions (0– 100°C for 30 and 120-min. cycle times; – 40–125°C for 42 min) were used. As a practical matter, the results of the 0–100°C ATC temperature range condition was considered to be of particular significance because it is the most widely used application range in computer, storage and network infrastructure/telecommunications systems which are the focus of this paper. For the 0–100°C/30-min. cycle, the slow-cooled 3.8Ag alloy exhibited the longest fatigue life, followed by the slow-cooled 2.1 and 2.5Ag alloys. The fast-cooled 2.1Ag joints exhibited the shortest fatigue life among the conditions tested (see Table 4). For the 120-min. cycle the trend was reversed, with the slow-cooled 2.1%-Ag joints exhibiting the longest fatigue life, followed by slow-cooled 2.5%-Ag and, fast-cooled 2.3Ag (and 0.2%-Bi) exhibiting the shortest fatigue life. In all cases, the number of cycles to failure decreased upon increasing the cycle time from 30 to 120 min, consistent with the prior study. This points to the fact that near-eutectic Sn–Ag solders require a much longer cycle time (i.e., stress relaxation period) in order for the maximum damage to occur, which is much longer than required for Sn–Pb solder joints. Accordingly, if the stress cycle used during ATC testing is too short, the results are likely to be more optimistic than those actually achieved under field conditions. It also implies that longer test-cycle times are necessary for meaningful Pb-free solder ATC testing in comparison to Pb–Sn solders. The Pb-free solder fatigue life values were even more drastically reduced for the – 40–125°C, 42-min stress conditions (Table 4) due to the larger temperature range ($\Delta T = 165$°C compared to 100°C) and higher peak temperature ($T = 125$°C). In essence, under these severe test conditions, the fatigue life of each test cell (i.e., solder alloy at a specific cooling condition) was observed to be only about 1/3 of its 0–100°C, 30-min condition fatigue life. This study further demonstrates the complexities involving the reliability of Pb-free solders, particularly the fatigue characteristics of near-eutectic Sn–Ag–Cu alloys. For example, based on the ATC data low-Ag content solder joints provide a superior thermal fatigue life in the case of 0–100°C, long-cycle time (120 min.) stress conditions, but not for short-cycle time, nor the – 40 to 125°C condition, for which the slow-cooled, high-Sn (3.8%) alloy was noted to perform best. This is in spite of the fact that the slow-cooled high-Sn joints were observed to contain large Ag_3Sn plates oriented in random directions, suggesting that other factors, such as the stress conditions may be more important than the presence of Ag_3Sn plates in determining solder-joint thermal fatigue life. Nevertheless steps to remove Ag_3Sn plates from a solder joint microstructure should be taken since their presence is believed to pose a reliability risk.

5.4 Benefits of low Ag

The benefit of reduced Ag content to avoid the formation of Ag_3Sn plates remains unclear. However, what is clear is that low-Ag joints have a much reduced fatigue life sensitivity to increasing cycle times. It

Table 4 Average fatigue life (N_{50}) determined from ATC failure data of Sn–Ag–Cu BGA solder joints and their ranking

Alloy composition (cooling rate)	ATC stress conditions					
	0–100°C		0–100°C		–40–125°C	
	(30 min)	Rank	(120 min)	Rank	(42 min)	Rank
Sn–3.8Ag–0.7Cu (Slow)	1,408	1	1,012	4	452	1
Sn–3.8Ag–0.7Cu (Fast)	1,164	5	982	5	392	4
Sn–2.5Ag–0.9Cu (Slow)	1,212	3	1,108	2	446	2
Sn–2.5Ag–0.9Cu (Fast)	1,200	4	1,054	3	384	5
Sn–2.5Ag–0.5Cu–0.2Bi (Slow)	1,212	3	953	6	407	3
Sn–2.5Ag–0.5Cu–0.2Bi (Fast)	1,130	6	934	7	376	6
Sn–2.1Ag–0.9Cu (Slow)	1,224	2	1,188	1	372	7
Sn–2.5Ag–0.9Cu (Fast)	1,064	7	1,012	4	384	5

After Ref. [36]

was observed that low-Ag solder joint fatigue life decreased less with increasing ATC cycle time in comparison to joints with higher Ag contents [36]. Low Ag content does provide a microstructure considered to be more favorable to enhancing fatigue life. Near-eutectic Sn–Ag–Cu alloys with reduced Ag contents have a lower volume fraction of eutectic constituents, a higher volume fraction of the *β*-Sn dendrite phase, and an increased Sn-dendrite size. These microstructural changes have been observed to result in decreased microhardness when Ag content is decreased [36]. The creep deformation of near-eutectic Sn–Ag–Cu alloys is understood to be mainly associated with the *β*-Sn phase rather than the eutectic constituents [37]. A coarse dendritic structure resulting from a reduced Ag content would be expected to exhibit an enhanced resistance to the creep component of thermal-cycle tests relative to similarly tested high-Ag joints.

In addition to being insensitive to cycle time, the thermal-fatigue life of low-Ag solder joints was also observed to be quite insensitive to cooling rate variations. This is a distinct advantage because they therefore are also less sensitive to variations in reflow process conditions during manufacturing. High-Ag content alloys such as Sn–3.8Ag–0.7Cu, exhibit high sensitivity to cooling rate variations [36].

The above fatigue studies demonstrate that Pb-free solder thermal fatigue behavior is very dependant on the test stress conditions and much more so than similarly tested Pb–Sn solders.

6 Tin crystal structure related anomalous behavior

There are fundamental crystalline structure differences between Pb and Sn that directly effect physical properties. At room temperature Sn exists as a body-centered tetragonal (BCT) crystal structure, referred to as white tin (*β*-Sn), compared to lead's face-centered cubic (FCC) structure.

The BCT Sn crystal structure is less symmetric than the face-centered cubic Pb structure and is, therefore, unable to as easily deform under stress. The BCT asymmetry also results in anisotropic physical properties like the CTE. Differences in CTEs between adjacent tin grains create grain-boundary stress when thermally cycled that can cause cracks to initiate at grain boundaries and may result in solder joint failure.

Yet another difference between Pb-bearing and pure Sn or some tin-rich solders is that the Sn-rich alloys undergo a phase change at 13.2°C which is in the middle of most ATC temperature extremes. When the temperature dips below 13.2°C tin changes from BCT

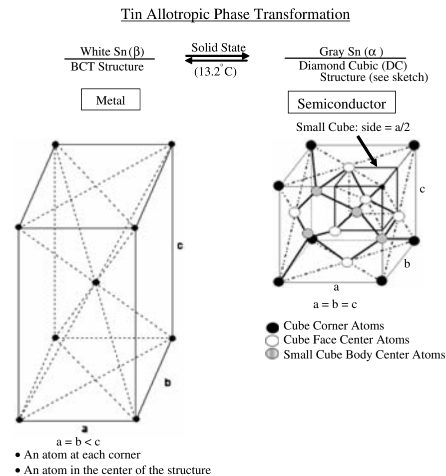

Fig. 11 Illustration depicting an allotropic transformation from a body-centered tetragonal (BCT) to diamond cubic (DC) crystal structure at 13.2°C

white-tin (*β*-Sn), with essentially metallic properties, to a diamond cubic (DC) structure gray tin (α-Sn) with essentially semiconductor characteristics (see Fig. 11). Because of the very brittle nature of gray Sn and the 21% increase in volume that accompanies the transformation, the material suffers a severe loss in structural integrity, and loss of thermo-mechanical fatigue resistance due to the build-up of internal stresses that result in fractures [38]. However, an extended period below 13.2°C is necessary to initiate the tin pest transformation. Consequently rapid temperature cycling does not result in transforming white Sn to gray Sn. But the transformation can occur in areas such as airplane storage areas where temperatures typically range between – 40 and 60°C. The surface has a rough appearance and contains many cracks (see Fig. 12). The *β*-Sn to α-Sn transformation also results in an approximately 25 times increase in electrical resistivity which is sufficient to cause failure in many sensitive high-performance electronic circuits. The adverse physical changes that accompany white tin's allotropic phase change to gray tin is referred to as tin pest. Tin pest has not been observed for all Pb-free solder candidates and finishes (e.g., the Sn–Ag–Cu alloys) but it has been observed in Sn–0.7Cu [38]. Although Sn-rich solders are prone to exhibit tin pest, minor additions of certain alloying elements, particularly Bi and Sb, have been proven to be effective in retarding the tin-pest reaction. Tin pest is one of the new concerns brought about by the use of Pb-free alloys that did not exist

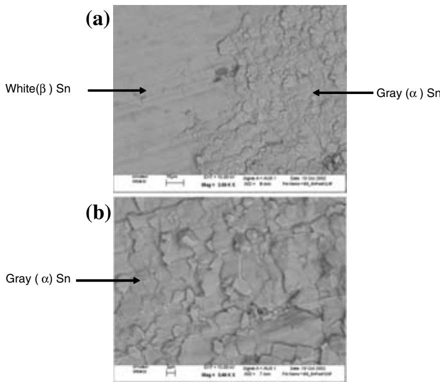

Fig. 12 Scanning electron micrographs of the surface of a Sn–Cu sample that has partially transformed from white (β) tin to gray (α) tin. (**a**) Right side of the photograph shows the rough surface of the transformed region (i.e., α-Sn) as contrasted with the smooth surface of the untransformed β-Sn on the left side. (**b**) An enlargement of the right side of (**a**), i.e., transformed to α-Sn (courtesy of IBM Corporation)

with the use of Sn–Pb solders in electronic products, because Pb is among those elements that resist the tin-pest transformation.

7 Tin-whisker issues and concerns

Metal whiskers are thin, hair-like single crystal filaments that erupt from a metal surface (Fig. 13) and can be straight, kinked and even curved. Some have a fluted surface, while others do not. Most, if not all non-noble metals grow whiskers under certain ambient or near-ambient conditions. However, the greatest focus is on whiskers that typically grow from tin-plated finishes due to their pervasive use in electronic assemblies. Whiskers grow in length over time, and can become several millimeters long. Because they are conductive, they can cause a number of failure conditions. In high-impedance, low-current circuits a whisker can cause a permanent short circuit which may require as much as 50 mA to "burn out". But whiskers can also cause temporary, or intermittent, shorts prior to being vaporized. Whisker vaporization can also cause serious problems. For example, in some space applications a whisker's vaporization can create a plasma with a current-carrying capacity of hundreds of amperes. Tin whiskers can also have an effect even when not causing short circuits. For example, in high-frequency RF (> 6 GHz) or in fast digital circuits (rise time < 59 ps), whiskers can act as a conductive stub (i.e., antennae) affecting circuit impedance and causing

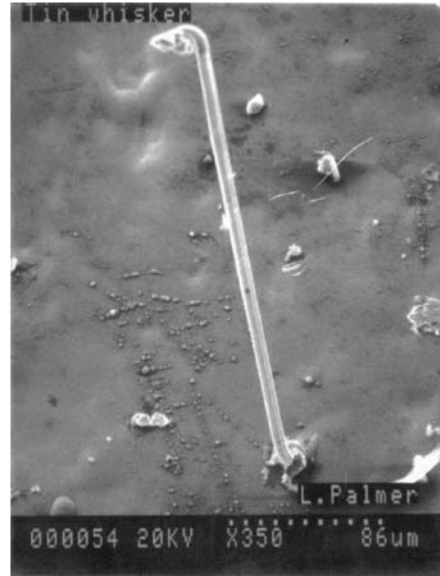

Fig. 13 A scanning electron microscope (SEM) image of a whisker that grew from a bright-tin plated film (after Ref. [39])

reflections. In electromechanical systems, such as disk drives, whiskers may break off and cause head crashes or contaminate bearing surfaces. Similarly they may contaminate the optics in electro-optical systems and reduce the effective isolation for high-voltage components in power-supply systems [40].

7.1 Tin plating types

There are several types of pure-tin plated coatings or finishes (Table 5). Each tin finish type has characteristics that result from plating conditions and the chemicals added to the plating bath. So-called bright tins are highly reflective due to their smooth texture and small grain size. They are often selected for connector applications because they possess good abrasion resistance and a lower coefficient of friction relative to other tin coating types. However, bright tins have a relatively high residual film stress and are more prone to whisker growth so they tend to be long (up to 5000 microns in length). Matte tins have a dull appearance because of their rough surface texture and larger grain size (typically > 5 μm). Matte tins are often utilized for PCB and component lead finish applications. Matte tins are much less prone to whisker growth than bright tins and rarely grow greater than 500 microns in length. Satin-bright films are intermediate in their appearance

Table 5 Common types of pure tin finishes and their characteristics

Sn plating	Appearance	Comments/characteristics
Matte tin	Dull appearance due to rough surface texture	Relatively large grains Typically μm Only Sn plating up to mid-1960s Large polygonal grains Usually extend through thickness of the film Achieved by organic additions to the bath Residual stress < bright Sn Grows whiskers but < density and smaller compared to bright Sn
Bright tin	Bright, highly reflective due to a smooth texture	Relatively small grain size Typically < 1 μm To achieve brightness add organic agents to plating bath Residual stress > matte Sn Whisker growth more prolific than matte Sn, longest whiskers
Satin bright tin	Brightness intermediate between matte and bright Sn	Stress is intended to be as close to zero as possible

between matte and bright tins and are designed to have a near-zero film stress. Tin plating has been the plating of choice throughout the electronics industry since the early 1950s. Around 1960 it became common practice to add lead (Pb) to electroplated tin films to enhance solderability and to mitigate whisker formation.

7.2 General areas of agreement

The European Union's ROHS regulations require that the lead (Pb) content be drastically reduced (to less than 1,000 ppm) which exposes the end user to whisker-related reliability failures due to whisker shorting. These reliability concerns have caused a flurry of research investigating whisker formation starting around 2000 and still in progress today. Whiskers have been a topic of scientific interest since about 1950 and there are a significant number of whisker-related studies described in the scientific literature [41]. The great majority of the published research concludes that compressive stress is the driving force for whisker formation and that whisker formation is one of several stress relieving mechanisms. The more recent research does not contradict these historical findings relative to compressive stress and the iNEMI (International Electrical Manufacturer Initiative) whisker modeling committee has taken the position that compressive stress is, beyond any reasonable doubt, the driving force for whisker formation and growth [42]. All published works agree that diffusion is the mechanism by which tin atoms move towards the whisker from adjacent regions, and most researchers believe that grain-boundary diffusion is the specific diffusion mechanism responsible for whisker growth. There is a (minority) body of opinion that holds surface diffusion to be at least partially responsible for some movement of tin atoms towards the whisker-growth site. All published researchers, without exception, acknowledge that whiskers grow from the addition of tin atoms to the base of the whisker and not from the addition of tin atoms to the growth tip [43]. There is little or no consensus on other aspects of whisker growth including recrystallization, creep, grain boundary slip, and dislocation mechanisms. Nevertheless, the basic tenet that whisker growth is one form of stress relaxation is generally accepted by the published research.

7.3 The role of recrystallization

Tin deformation has long been known [44] to accelerate whisker formation, and if a deformation stress is maintained through a clamping action the whisker growth rate is accelerated by several orders of magnitude. A pure clamping action without deformation does not appear to accelerate whisker formation [45]. When the clamping action results in plastic deformation it is observed that whiskers form at an accelerated rate from the deformed material. Focused ion beam (FIB) examinations of whiskers growing from deformed material has shown that extensive recrystallization occurs within the mass of the deformed material and that whiskers grow from a grain (i.e., a whisker grain) which is itself unique in morphology with respect to both other recrystallized grains and the parent grain structure of the as-deposited film [46]. This unique morphology can best be described as a set

of oblique (i.e., at an angle), relatively straight-sided, grain boundaries that intersect the surface at angles between 30 and 60°. In cases involving deformed tin, it is highly likely that whisker grains result from a recrystallization event that itself was the result of tin deformation. These straight-sided, oblique-angle whisker grains are always observed with whiskers no matter what the circumstances. However, for matte and satin-bright tins without a clear deformation event the oblique-angled whisker grains are not associated with an obvious recrystallization event. Instead, the matte/satin-bright whisker grains appear to form directly from the columnar-grain structure of the as-deposited tin. Most researchers acknowledge that the deformation events and the whiskers that form from very-bright tins involve a recrystallization event, but there is no agreement on whether recrystallization events play a role in whisker formation from matte and satin-bright tin films.

7.4 Problematic conditions

A variety of practices and environmental conditions have been identified that are known to exacerbate whisker formation. For example, copper readily co-deposits with electrolytic tin and forms Cu_6Sn_5 intermetallic particles that are dispersed throughout the tin matrix. It has long been known that the introduction of copper to a tin film in amounts ranging upwards of approximately 100 ppm greatly increases the tendency to nucleate and grow tin whiskers. It appears that copper alloying increases the built-in compressive stress state of the film and, thereby, increases the probability of whisker formation [47]. Unfortunately, copper may be present in a tin film even when it is not specifically requested. One of the authors (G. Galyon) has dissected many supposedly pure-tin films and found that they contain significant amounts of copper. Invariably, these copper-containing tin films were observed to have tin-whisker formation problems. Temperature cycling is also known to add stress to tin films and accelerates whisker formation. In fact, many whisker researchers utilize temperature cycling to induce whisker formation. The difference in the CTE between the deposited-tin film and the base metal upon which it is deposited (i.e. substrate) is the direct cause for the stress buildup that occurs during temperature cycling. Temperature-cycling induced stresses are particularly problematic for tin films deposited on Alloy42 (Fe42Ni) substrates due to the large CTE differences between film and substrate (23 vs. 10 ppm, respectively). High-humidity environments (typically > 85% RH) accelerate whisker formation. The iNEMI group investigating Sn-whisker formation capitalized on the concept by utilizing a combination of temperature cycling and high humidity environments [48] to induce whisker formation. Their analysis showed that high-humidity environments not only increase the average surface oxide thickness, but that the conversion to tin oxide can, in some localized areas, extend from the film surface down to the film/substrate boundary. Oxide formation should, and apparently does (although no direct data exists confirming this fact), add to the compressive stress state and, thereby, accelerates whisker formation. Interestingly, tin deposited on copper or copper-alloy base metal surfaces that experience temperature cycling or temperature storage in the absence of high humidity results in the formation of pedestals. Pedestals are individual grains that are converted entirely to a copper–tin intermetallic compound (Cu_6Sn_5). Pedestal grains are observed to be scattered throughout the matrix of pure-tin, columnar-like grains. The pedestals form because for some unknown reason(s) certain tin grains appear to have anomalously high bulk diffusion parameters for Zn, Cu, and oxygen so they are readily oxidized or diffused. Consequently these "special" grains form what are termed as pedestals [46, 49].

Brass (Cu–Zn) surfaces are the most prone to tin whisker formation. Zinc is an extremely fast diffuser in tin and diffuses from the brass substrate to the tin-film surface in significant quantities very soon after deposition. A common mitigation practice for tin-plated brass substrates is the use of a copper underlay > 1.0 micron in thickness. However, the basis for the effectiveness of a copper underlay is not understood since there are no known studies that have addressed this matter.

Tin-plated steel for cabinets and drawers is relatively rare today. Zinc coatings are currently the finish of choice for the steel sheet-metal industry. Tin whisker formation is accelerated when steel substrates are not adequately cleaned. The belief is that a rusty (i.e., oxidized) steel surface induces stresses within the deposited tin film to promote whisker formation.

7.5 Mitigation practices

Whisker prevention (mitigation) in tin and tin-alloy films is largely based on stress reduction. There are no absolute preventative techniques. The objective is to mitigate, or lessen the probability of whisker growth. Several mitigation techniques that have been practiced are noted in Table 6.

Table 6 Tin-whisker mitigation practices

Practice	Comments
Alloying	
With Pb	Banned by EU as of 7-1-06
With Ag, Bi	Rarely practiced, supported by iNEMI
Fusing	Melt the Sn film, slowly cool to relieve stresses
	Rarely practiced
Annealing	Typically heat to 150°C, 1 h
	Widely practiced, supported by iNEMI
Use of underlay films	Thin film between the base metal and Sn-film layer
Nickel (Ni)	Widely practiced by connector companies, supported by iNEMI
Silver (Ag)	Rarely practiced
Copper (Cu)	Rarely practiced
	Utilized for Sn films deposited on brass base-metal surfaces
Pure tin plated films	
Matte Sn	Widely practiced
	Not supported by iNEMI, controversial
Satin bright tin	Rarely practiced
	A lower stress variant of bright Sn

These mitigation techniques are intended to modify the tin stress state and so reduce and/or eliminate tin-whisker formation. Each technique has some supporting data. However, it is also true that not all the experimental data supports the effectiveness of each mitigation technique noted. Each mitigation technique has its strength and weakness. The effectiveness of several of these techniques is very dependent on proper procedure and practice. Consider, for example, underlays (whether copper, nickel, or silver) which must be thick enough to provide good coverage of the underlying base material. If the underlay is too thin the tin film will come into direct contact with the copper base metal at point locations, thereby negating the mitigating effect of the underlay material. Typically underlay thickness of > 1.0 micro meter are necessary to be effective, a greater thickness may be necessary in cases of surfaces with a high surface roughness.

The potential for tin whisker formation on tin-rich finishes and the reliability risk they pose is too great to recommend using these finishes in life-threatening applications such as heart pacemakers or military avionics. However, the reality is that manufacturers of these and high-performance electronic products will sometimes not have the ability to procure components with non-tin based finishes. In these cases the authors recommend that mitigation practices be adopted that best minimizes the risk of whisker formation and growth.

8 Electromigration concerns

There are several physical processes that can cause solder joint mechanical and electrical properties to degrade. One of these physical processes is electromigration. Electromigration is a mass transfer phenomenon resulting from the momentum-transfer between moving electrons and the constituent atoms in the conducting material. Electromigration is of particular concern for flip-chip solder joints because of the strong demand for continually increasing power levels and ever-smaller solder joints. Current densities in flip-chip solder joints are anticipated to soon reach $\sim 2.74 \times 10^3$ A/cm^2, a level at which there is concern for failures due to electromigration [50].

Conducting electrons are believed to collide with diffusing metal atoms that are then pushed in the direction of the electron flow as a result of those collisions. The phenomenon can occur with any current carrying metal but it is usually negligible and can safely be ignored. It becomes a consideration in cases where the diffusion rates are relatively rapid and the current density is high; conditions not unusual for advanced semiconductor devices and their flip-chip terminations as utilized in high-performance electronic equipment. "Effective charge" is a quantity that relates how diffusing atoms interact with or absorb the impact of conducting electrons, which itself is a complex function of a metal's atomic structure and is directly related to the driving force for electromigration. For solder materials, including tin, the effective charge is relatively high [51]. Other important electromigration factors are resistivity and current density. Conductor lines or terminations consisting of material with a combination of a high effective charge, one or more fast diffusing elements, and experiencing a high current density is a candidate for electromigration effects and potential catastrophic failure.

8.1 Fast diffusers

Copper (Cu), silver (Ag), gold, (Au), and nickel (Ni) are rapid diffusion elements in both Pb and Sn. These elements are routinely utilized in electronic assemblies for integrated circuits, printed circuit boards (PCBs), and solder joint terminations including the under-bump metallization (UBM) of flip-chip solder joints. They also frequently form IMCs with Sn. Fast diffusers occupy interstitial sites in the host-metal lattice. Lead

(Pb) has a close packed, FCC lattice, whereas tin's body-centered tetragonal lattice (BCT) is not close packed. Both Pb and Sn are large atoms and consequently contain relatively large interstitial sites that easily accommodate the much smaller noble and near-noble metal atoms. Accordingly, it has been determined that these smaller atoms diffuse interstitially in Pb and Sn and do not require vacancies in order to jump (i.e., diffuse) [51].

8.2 Electromigration failure in flip-chip solder joints

Electromigration effects in flip-chip solder joints usually result from the mass transport of a major solder species (i.e., Pb) or alloying element. It is also possible to have electromigration failures due to the mass transport of a minor, fast-diffusing species.

8.2.1 Solder-related failure

Flip-chip, solder-joint electromigration failures where the mass transport involves a major constituent are usually the result of void formation. Large voids cause a significant increase in electrical resistance with an associated increase in temperature eventually leading to an open circuit. Surface extrusions can also be created by electromigration that cause short circuits [52–54]. A shallow void is often formed with a lenticular shape (Fig. 14), located at the interface of the solder and IMC associated with the UBM terminal metal. The geometry of flip-chip solder joints at the capture pad and narrow chip-via region (Fig. 15) causes current crowding, resulting in high local current densities, about 50 times greater than the solder bump [55, 56]. The condition also causes the generation of heat (i.e., increased temperature) that further exacerbates the situation. This is the mode of failure often observed when the direction of electrical current flow is from the chip to the chip carrier (Fig. 16a). But if the current density is sufficiently high when the direction of current flow is from the chip carrier to the chip, failure can occur at the chip-carrier side of the solder joint as well (Fig. 16b).

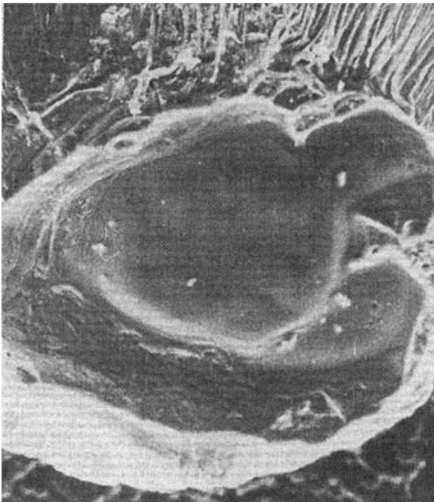

Fig. 14 Scanning electron microscope (SEM) image that shows the smooth surface characteristics of a lenticular-shaped void that often involves the entire cross section of the chip via in electromigration failures of flip-chip solder joints (after Ref. [51])

8.2.2 UBM-related failure

Electromigration failures can also involve degradation of the underbump metallurgy (UBM) structure for flip-chip solder joints; particularly if fast-diffuser elements are incorporated in the structure. Fast diffusers result in UBM dissolution and stress generation due to excessive IMC formation that causes interfacial fracture, and ultimately circuit failure [55, 57].

8.3 Electromigration in lead (Pb)-free solders

Electromigration data related to Pb-free solders is sparse. It is known that Sn acts much like Pb as a host for fast diffusers. Metals that diffuse rapidly in Pb also diffuse rapidly Sn. But there are some important differences between Pb and Sn with respect to diffusion. One of the most important differences is due to tin's BCT lattice structure which results in anisotropic diffusion properties. For lead (Pb) the diffusion

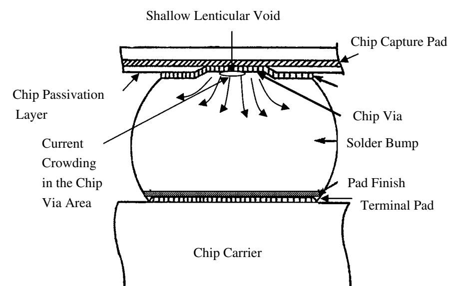

Fig. 15 Illustration depicting some aspects often associated with electromigration failures in flip-chip solder joints

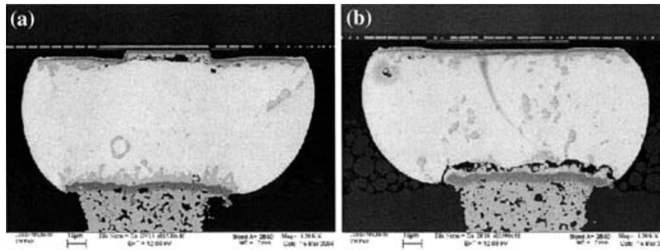

Fig. 16 Photomicrographs of vertical cross sections of lead-free flip-chip solder joints that have failed due to thermomigration during testing. (**a**) Failure occurred near the chip via, the direction of electrical current flow was from the chip to the chip carrier. (**b**) Failure occurred near the chip carrier, the direction of electrical current flow was from the chip carrier to the chip. (Courtesy of H. Longworth, IBM Corporation)

coefficient is independent of orientation, but not so in tin where the diffusion coefficients are very different for directions parallel ("*a*" direction) and perpendicular ("*c*" direction) to the basal plane. This is also true for self-diffusion. In the case of fast diffusers in tin, the ratio of the *a*/*c* diffusion coefficient varies by a factor of 30–50 at 200°C [51]. A greater variation in electromigration susceptibility may, therefore, be anticipated among Pb-free solder joints due to these diffusion coefficient orientation dependencies and the fact that flip-chip solder joints typically consist of very small numbers of individual grains (usually < 10). Electromigration test results for Pb-free flip-chip solder joints have been quite favorable in comparison to eutectic Sn–Pb. For example, in a test consisting of commercially available electroplated Sn–Ag solder bumps with a Ti/Cu/Ni UBM the data showed an electromigration lifetime one order of magnitude greater in comparison to eutectic Sn–Pb bumps at constant currents up to 800 mA and temperatures up to 165°C [58]. High-performance electronic circuits utilize high-Pb (i.e., 97Pb–3Sn) solder to benefit from both the superior electromigration and fatigue resistances exhibited by this material [59]. Another study was conducted [50] comparing the electromigration resistance of Sn–3.5Ag and 90Pb–10Sn flip-chip solder joints at similar current density levels (3.5 and 4.1×10^4 A/cm^2). However, a different set of temperatures were selected close to the melting temperature of the test solders in an attempt to hasten the failure process (185 and 202°C for high Pb; 122 and 155°C for Pb-free). The high-Pb solder joints exhibited an electromigration lifetime approximately four times longer than the Pb-free joints in spite of being tested at a much higher temperature. The Pb-free solder joints performed better than the eutectic Sn–Pb solder joints investigated in the study cited earlier [59]. Flip-chip solder joint dimensions are steadily decreasing in response to the need for higher input–output (I/O) densities. At the same time, flip-chip solder joints used in high-performance equipment are experiencing ever higher current levels which are soon expected to be 0.3–0.5 A or more per solder joint [57, 60]. Although the available reliability data is meager, what is available raises disturbing concerns as to whether Pb-free solders possess the necessary electromigration (EM) resistance. Even at present current-density levels it appears the reliability risk for lead-free solders is too great. These reliability issues require a much better understanding before Pb-free solders can be relied upon to provide a safe level of EM resistance.

9 Summary/conclusions

This paper has discussed the major technological issues impeding implementation of Pb-free solder materials for high-performance electronic systems (i.e., servers, storage, network infrastructure/telecommunications systems) due to their potential negative reliability impact. It was concluded that:

(1) The solder wetting characteristics of all the major Pb-free solders currently under consideration are worse than eutectic Sn–Pb; some of the Pb-free solders are significantly worse than eutectic SnPb. The actual reliability impact of lead-free solder implementation is not well understood, but it is generally agreed that sound solder joints can be made with Pb-free solder. However, the process window for the formation of acceptable Pb-free solder joints is more restricted given the higher melting points for most of these materials.

(2) The large degree of undercooling required to nucleate the β-Sn phase in Sn–Ag–Cu alloys gives rise to a highly non-equilibrium structure in relation to that predicted by the phase diagram. In addition, under slow cooling conditions from

the melt, very large randomly oriented Ag_3Sn platelets are formed throughout the solder joint. There is some controversy as to whether these platelets have an adverse affect on reliability. It is generally felt that the Ag3Sn platelets are a reliability risk and their formation can be greatly reduced and even eliminated by reducing the Ag content to approximately 3% or less.

(3) The fatigue characteristics of the major Pb-free solder candidates (SAC, SAB) are very dependant upon test or application conditions (i.e., peak temperature, temperature range), and the cooling rate during the solder attachment process. Under some conditions the fatigue resistance of SAB and SAC is superior to eutectic Sn–Pb; for others it is approximately equivalent or markedly worse. The stress-relaxation time constants for SAC and SAB solders are far longer than those for eutectic Sn–Pb. As a result, ATC tests whose cycle times are too short will predict an overly optimistic field life. It should be apparent from these discussions that longer test times will be required to adequately characterize Pb-free solders. Consequently, due to these additional complications much more needs to be done to fully understand the very important issue of thermomechanical fatigue resistance in Pb-free solder joints.

(4) Tin's BCT crystal structure gives rise to anisotropic properties including the CTE, which is expected to have a negative impact on flip-chip solder joint reliability because they consist of few grains (~10). The BCT structure is also less capable of dissipating stress compared to lead's FCC structure and so maintains higher stress levels for longer periods of time. Tin also transforms to a very brittle DC structure when cooled below 13.2°C and this phase change results in a complete loss of structural integrity and a large increase in electrical resistivity. The condition is known as tin pest and is one that pure tin and tin-rich solders are particularly susceptible to, but not Pb–Sn solders.

(5) Fine, hair-like filaments referred to as tin whiskers that can form on pure Sn or Sn-rich finishes and often utilized on component lead frames can cause electrical shorts and numerous other problems. Although the industry has defined several mitigation practices that all serve to reduce risk, none of them is an absolute guarantee to halt whisker formation. Until one is determined, tin-whisker formation will continue to be a major concern for high-performance systems.

(6) With the continuous reduction in solder joint cross sections, particularly those of flip-chip solder joints, and the need for them to support higher electrical current levels, resulting in higher current densities, it is questionable whether Pb-free solders are capable of reliably performing their current-carrying task without degradation due to electromigration. It is not sufficient that they appear to possess better thermomigration characteristics compared to eutectic Sn–Pb. Only high-Pb solders appear to possess both the necessary thermal fatigue and thermomigration properties necessary to meet flip-chip solder joint requirements.

In consideration of the findings in relation to all the key issues discussed, it is concluded that the solder exemption accorded to high-performance systems was both necessary when granted by the EC and most likely will require an extension when reviewed in 2008, and perhaps well into the future.

References

1. Military and Obsolete Components—ROHS Directive, Dionics, Dec. 29, 2005. http://www.high-rel.com/rohs.htm
2. R.D. Hilty, ECN, Nov. 1, 2005. http://www.ecnmag.com/article/CA6279217.html
3. J.F. Mason, Electronic News, Dec. 22, 2005. http://www.read-electronics.com/electronicnews/index.asp?layout=articleprint&articleID
4. S. Deffree, Electronic News, Dec. 23, 2005. http://www.read-electronics.com/electronicnews/index.asp?layout=articlePrint&articleID
5. B. Dastmaichi and R. Vermeij, Transition to ROHS: the seven common pitfalls to avoid, Nov. 11, 2005
6. R.D. Hilty and M.K. Myers, Tyco electronics publication 503–1001, 2004, Revision 0
7. Implementation of Lead-free Packages, Spansion, 2005, http://www.spansion.com/support/lead_free_flash/Lead_Free_Packages.html
8. Backward and Forward Compatibility, Dallas Semiconductor, http://www.maxim-ic.com/emmi/backward_forwards_compatibility.cfm
9. R. Rowland, Surface Mount Technology, Nov. 2005, http://www.surfacemount.printthis.clickability.com/pt/cpt?action=cpt&title=surface+Mount+TEC
10. A. Maheshwari, Xcall Journal, Summer 2004, abhay.maheshwani@xilinx.com
11. Lead Free and ROHS Data, Freescale Semiconductor, 2004/2005, http://www.freescale.com/wehap/sps/site/overview.jsp?nodeId=061R7NMSSR
12. F. Hua, R. Aspandiar, T. Rothman, C. Anderson, G. Clemons, M. KLIER, in *Proc. Surface Mount Technol. Assoc. (SMTA) International Conf.*, Sept. 22 (2002)
13. F. Hua, R. Aspandiar, C. Anderson, G. Clemons, C. Chung, M. Faizul, in *Proc. Surface Mount Technology Assoc. (SMTA) International Conf.*, Sept 21, (2003), pp. 246–252

14. S. Bagheri, P. Snugovsky, Z. Bagheri, M. Romansky, M. Kelly, M. Cole, M. Interrante, G. Martin, C. Bergeron, in *Proc. CMAP International Conf. on Lead-free Soldering*, (May, 2006), Toronto, Canada
15. P. Snugovsky, M. Kelly, A. Zberzhy, M. Romansky, in *Proc. CMAP International Conf. on Lead-free Soldering*, May, 2005, Toronto, Canada
16. Impact to Customers: Forward/Backward Compatibility, National Semiconductor, http://www.national.com/packaging/leadfree/impact.html
17. K.J. Puttlitz, in *Handbook of Lead-Free Solder Technology for Microelectronic Assemblies*, eds. by K.J. Puttlitz, K.A. Stalter (Marcel Dekker, Inc, New York, 2004), pp. 239–280
18. S.K Kang, Ibid, 281–300
19. P.T. Vianco, Ibid, 167–210
20. W. Feng, C. Wang, M. Morinaga, J. Electron Mater. **3** 185 (2002)
21. C.A. Drewin, F.G. Yost, S.J. Sackinger, J. Kern et al. Sandia report, SAND 95–0196. UL-704, Sandia National Laboratories, Feb. 1995
22. P.T. Vianco, F.M. Hosking, J.A. Regent, in *Proc. NEPCON West 1992* (Des Plaines, IL), pp. 1730–1738
23. J.M. Tsung-Yu Pan, H.D. Nicholson, R.H. Blair et al., in *Proc. 7th International SAMPLE Electronics Conf.* (Parsippany, NJ, June 1994), pp. 343–354
24. T.J. Singler, S.J. Meschter, J. Spalik, in *Handbook of Lead-free Solder Technology for Microelectronic Assemblies*, eds. by K.J. Puttlitz, K.A. Stalter (Marcel Dekker, Inc., New York, 2004), pp. 331–429
25. K.W. Moon, W.J. Boettinger, U.R. Kitten, F.S. Biancaniello and C.A. Handwerker, J. Electron. Mater. **29**(10), 1122 (2000)
26. M.E. Loomans, M.E. Fine, Metall. Mater. Trans. A, Phys. Metall. Mater. Sci., **31A**(4), 1155 (April 2000)
27. D.W. Henderson, J.J. Woods, T.A. Gosselin, J. Bartelo et al., J. Mat. Res. **19**(6), 1608 (2004)
28. D.W. Henderson, T. Gosselin, A. Sarkhel, S.K. Kang, W.K. Choi, D.Y. ShIH, C. Goldsmith, K. Puttlitz, J. Mater. Res. **17**(11), 2775 (2002)
29. K.S. Kim, S.H. Huh, K. Suganuma, Mater. Sci. Eng. A **333**, 106 (2002)
30. D.R. Frear, J.W. Jang, J.K. Lin, C. Zhang, J. Minerals, Metals, Mat. Sci. (JOM) **53**(6), 28 (2001)
31. S.K. Kang, W.K. Choi, D.Y. Shih, D.W. Henderson, T. Gosselin, A. Sarknel, C. Goldsmith and K.J. Puttlitz, in *Proc. of 53rd Electronic Components and Technology Conference* (New Orleans, LA, May 2003), pp. 64–70
32. S.K. Kang, P.A. Lauro, D.Y. Shih, D.W. Henderson, K.J. Puttlitz, IBM J. Res. Dev. **415**, 607 (2005)
33. A. Woosley, G. Swan, T.S. Chong, L. Matsushita, T. Koschimieder, K. Simmons, in *Proc. Electronics Goes Green: Fraunhoffer Institute, Berlin, Germany* (Sept. 2000)
34. S. Prasad, F. Carson, G.S. Kim, L.S. Lee, A. Garcia, P. Rouband, G. Henshall, S. Kamath, R. Herber, R. Bulwith, in *Proc. SMTA Internat. Conf.* (Chicago, IL, Sept. 2000), pp. 272–276
35. J. Bartelo, S. Cain, D. Caletka, K. Darbha, T. Gosselin, D.W. Henderson, D. King, K. Knadle, A. Sharkel, G. Thiel, C. WoychiK, D.Y. Shih, S.K. Kang, K.J. Puttlitz, J. Woods, in *Proc. of APEX 2001* (San Diego, CA, Jan, 2001), 14–18, LF2–2, 1–12
36. S.K. Kang, P. Lauro, D.Y. Shih, D.W. Henderson, J. Bartelo, T. Gosselin, S.R. Cain, C. Goldsmith, K.J. Puttlitz, T.K. Hwang, W.K. Choi, Mater. Trans. (Jpn. Inst. Metals) **45**(3), 695 (2004)
37. J.W. Morris, H.G. Song, F. Hua, in *Proc. 53rd Electronic Components Technology Conf.*, (New Orleans, LA, May 2003), pp. 54–57
38. M.J. Sullivan, S.J. Kilpatrick, in *Handbook of Lead-free Solder Technology for Microelectronic Assemblies*, eds. by K.J. Puttlitz, K.A. Stalter (Marcel Dekker, Inc., New York, 2004), pp. 915–978
39. W.J. Choi, G. Galyon, K.N. Tu, T.Y. Lee, IBID, 851–913
40. R.A. Quinnell, Test and Measurement World, 9–1-2005, http://www.tmworld.com
41. G.T. Galyon, IEEE Trans. Electr. Packag. Manufact. **1**, 94 (2005)
42. Meeting, International Electrical Manufacturers' Initiative (iNEMI) Whisker Modeling Committee, Herndon, VA, November 2005
43. S.E. Koonce, S.M. Arnold, J. Appl. Phys. **3**, 365 (1953)
44. R.M. Fisher, L.S. Darken, K.G. Carroll, Acta Metal. **3**, 368 (1954)
45. B.D. Dunn, European Space Agency (ESA) Report, STR-223, September 1987
46. G. Galyon, L. Palmer, IEEE Trans. Electr. Packag. Manufact. **1**, 17 (2005)
47. W.J. Boettinger, C.E. Johnson, L.A. Bendersky, K.W. Moon, M.E. Williams, G.R. Stafford, Acta Mater. **11**, 5033 (2005)
48. N. Vo, M. Kwoka, P. Bush, IEEE Trans. Electr. Pkg. Mfg., **1**, 7 (2005)
49. S.C. Britton, M. Clarke, in *Proc. 6th Internat. Metal Finishing Conf.*, May 1964, pp. 205–211
50. P. Su, M. Ding, T. Uehling, D. Wonton, P.S. HO, in *Proc. 55th Electronic Components & Technology Conf.*, (Lake Buena Vista, FL, May 31–June 3, 2005), pp. 1431–1436
51. J.R. Lloyd, K.N. Tu, J. Jaspal, in *Handbook of Lead-free Solder Technology for Microelectronic Assemblies*, eds. K.J. Puttlitz, K.A. Stalter (Marcel Dekker Inc., New York, 2004), pp. 827–850
52. C.T. Liu, C. Chen, K.N. Tu, J. Appl. Phys. **88**, 5703 (2000)
53. S. Brandonburg, S. Yeh, in *Proc. Surface Mount Internat. Conf. and Exposition* (San Jose, CA, 1998), pp. 337–344
54. T.Y. Lee, K.N. Tu, S.M. Kuo, D.R. Frear, J. Appl. Phys. **89**, 3189 (2000)
55. T.Y. Lee, K.N. Tu, D.R. Frear, J. Appl. Phys. **90**, 4502 (2001)
56. S.Y. Yang, J. Wolf, W.S. Kwon, K.W. Park, in *Proc. 52nd Electronic Components and Technology. Conf.* (San Diego, CA, 2002), pp. 1213–1230
57. M. Ding et al., in *Proc. Electronic Components and Technology Conf.* (Las Vegas, NV, June 1–4, 2004), pp. 968–973
58. B. Ebersberger, R. Bauer, L. Alexa, IBID, 683–691
59. J.D. Wu, P.J. Zheng, C.W. Lee, S.C. Hung, J.J. Lee, in *Proc. 41st IEEE Internat. Rel. Physics Symp*. (Dallas, TX, 2003), p. 132
60. Y.C. Hu et al., J. Mat. Res. **11** 2544 (2003)